

Turbulent flow and energy dissipation in plunge pool of high arch dam*

Écoulement turbulent et dissipation d'énergie dans la cuvette de déversement des grands barrages-voûtes

XU WEILIN, LIAO HUASHENG, YANG YONGQUAN and WU CHIGONG, *State Key Hydraulics Laboratory of High Speed Flows, Sichuan Union University, Chengdu, 610065, P. R. China*

ABSTRACT

The 3-D flow fields in the plunge pools of the Xiaowan high arch dam and Laxiwa high arch dam in China are simulated by the turbulence mathematical model and measured by the five-hole Pitot sphere combined with the pressure sensors and automatic data sampling and processing system. The typical 3-D flow pattern and energy dissipation characteristics in plunge pool are obtained. The simulated results of energy dissipation show that the water body in plunge pool can be divided into three regions: shear, impact and mixing dissipation regions of energy.

RÉSUMÉ

Les champs de courant 3-D dans les cuvettes de déversement des barrages-voûtes de Xiaowan et de Laxiwa en Chine sont calculés avec un modèle mathématique turbulent et mesurés au moyen d'une sphère de Pitot à cinq trous combinée à des capteurs de pression et un système d'échantillonnage et de traitement automatique. On obtient la configuration typique de l'écoulement 3-D et les caractéristiques de la dissipation dans la cuvette. Les résultats calculés de la dissipation d'énergie montrent que la masse d'eau dans une cuvette peut être divisée en trois régions: cisaillement, impact et mélange pour la dissipation d'énergie.

Introduction

Investigating the flow field of plunge pool is the basis of an in-depth study of the energy dissipation problem of plunge pool. However, the flow features of plunge pool have not been understood fully up to now. Practically no numerical simulations have previously been obtained (especially the 3-D numerical simulation), but also the 3-D flow field has not been previously measured in a physical model. In fact, it is the combination of numerical and experimental methods that is effective in the research of such complicated flow as plunge pool.

The Xiaowan hydropower station and the Laxiwa hydropower station are large-scale projects at the planning stage, which have high water head and large discharge. The Xiaowan hydropower station is located at the Lanchang River in southwest China. Its arch dam is 292m high. The maximum fall height and the flow rate through the dam are 226m and 15460m³/s respectively. The length of the plunge pool is 397m. The Laxiwa hydropower station is located at the Yellow River. Its arch dam is 250m high. The maximum fall height and the flow rate through the dam are 208m and 5783m³/s respectively. The length of the plunge pool is 244m.

1. Mathematical model

The main mathematical models of turbulent flow include the k-ε model,¹ the Reynolds stress model (differential or algebraic, i.e. RSM or ASM),² and the large eddy simulation (LES).³ In this paper, the 3-D k-ε model is employed to simulate the flow fields in the plunge pools. This choice is based on the following reasons: (1) It models the large flow structures satisfactorily. The small scale turbulence is less important; (2) The 2-D numerical simulation of the flow fields of plunge pools shows that the k-ε

model can give satisfactory results^{4,5} (the 3-D comparison between the calculated and the measured results will be described later in this paper); (3) Its results have been accepted by many hydraulic engineers and applied in the designs of some large-scale hydropower stations, e.g. Xiaowan,⁶ Laxiwa,⁷ Xiluodu⁸ and Ertan⁹ in China; (4) It is relatively simple.

The basic equations of the k-ε model are as follows:

continuity equation

$$\frac{\partial U_i}{\partial x_i} = 0 \quad (1)$$

momentum equations

$$U_i \frac{\partial U_j}{\partial x_i} = -\frac{1}{\rho} \frac{\partial p}{\partial x_j} - \frac{\partial(\overline{u_i u_j})}{\partial x_i} \quad (2)$$

k-equation

$$U_i \frac{\partial k}{\partial x_i} = \frac{\partial}{\partial x_i} \left(\frac{\nu_t}{\sigma_k} \frac{\partial k}{\partial x_i} \right) + \nu_t \left(\frac{\partial U_i}{\partial x_j} + \frac{\partial U_j}{\partial x_i} \right) \frac{\partial U_i}{\partial x_j} - \epsilon \quad (3)$$

ε-equation

$$U_i \frac{\partial \epsilon}{\partial x_i} = \frac{\partial}{\partial x_i} \left(\frac{\nu_t}{\sigma_\epsilon} \frac{\partial \epsilon}{\partial x_i} \right) + C_{\epsilon 1} \frac{\epsilon}{k} \nu_t \left(\frac{\partial U_i}{\partial x_j} + \frac{\partial U_j}{\partial x_i} \right) \frac{\partial U_i}{\partial x_j} - C_{\epsilon 2} \frac{\epsilon^2}{k} \quad (4)$$

where U_i , p , k and ϵ are respectively the time-averaged velocities,

Revision received May 8, 2001. Open for discussion till December 31, 2002.

* Sponsored by the National Natural Science Foundation.

time-averaged pressure, turbulent energy and its dissipation rate. The Reynolds stresses are calculated by the eddy-viscosity assumption. The eddy-viscosity coefficient $\nu_t = C_\mu k^2/\epsilon$. The constants C_μ , $C_{\epsilon 1}$, $C_{\epsilon 2}$, σ_k and σ_ϵ are respectively equal to 0.09, 1.44, 1.92, 1.0 and 1.3. The discretization forms of the above-mentioned equations are derived by using the control-volume method. The discretization of the convection and diffusion term is achieved in terms of the power-law scheme. The SIMPLER algorithm is employed in the calculation of the velocity and pressure fields. For the slope boundary, the nodes under the inclined plane are "blocked-off", i.e. letting $S_p = -10^{30}$ and $S_c = 0$ in the source terms (written as $S_\Phi = S_p\Phi + S_c$, where S_Φ is the source term and Φ is the general variable) of the above-mentioned equations at those nodes so that all of the variables are equal to zero in the blocked-off regions throughout the numerical calculation. The calculation is achieved by a Compaq professional workstation. The run-time is usually 12~18 hours. The numerical stability needs to be controlled carefully by changing the under-relaxation factors. No numerical diffusion is found. The averaged grid size is about 2 cm in the physical model approx $4m \times 0.8m \times 0.4m$. The number of grid points is $200 \times 40 \times 17$. The inflow velocity and the inflow jet width are from the experimental data of the physical model. The inflow jet thickness is calculated by the flow rate, the

velocity and the width. The calculated inflow jet thickness is approximately equal to the averaged one of an inflow jet in the physical model, where the jet is not spread very much in the atmosphere. On the free surface, the normal velocity component and the normal gradients of other variables are equal to zero. On the wall boundary, the Wall-Function method¹ is adopted.

The flows in plunge pools are very complex. Obviously, it is very difficult to simulate all flow phenomena. In fact, in the design of plunge pools, the pressure on the floor is the most important parameter and followed with interest by engineers. The influence of aeration on the pressure on the plunge pool floor has been investigated experimentally by Dong et al.,¹⁰ whose results show that the influence is small. Therefore, the entrained air bubbles are not considered in the numerical simulation. Some experimental investigations on the aerated flows in plunge pools can be seen in the papers of Mason,¹¹ Ervine, Falvey and Withers,¹² Ervine and Falvey,¹³ McKeogh and Elsayw,¹⁴ etc.

To show the turbulence model is suitable to simulate the flow in plunge pools, an example of the comparison between the measured and the calculated pressure distributions on the pool floor is given in Fig.1. It can be seen that they are in good agreement.

2. Experimental method

The intense turbulence and aeration make it very difficult to measure the flow field in the plunge pool. In view of the flow characteristics in the physical model, a five-hole Pitot sphere is used as velocity measurement instrument, by which the 3-D velocities can be measured at the same time. Fig.2 is the sketch of the five-hole Pitot sphere. The diameters of the Pitot sphere and its pressure holes are respectively 5mm and 0.35mm. In experiment, the pressure sensors are connected to each pressure hole by pipes. The hydrodynamic pressure in each hole is transformed into electric signal and transmitted to the automatic data sampling and processing system. These devices, together with a microcomputer, allow the measurement to be taken automatically.

Because the pressure holes of the Pitot sphere are connected to the pressure sensors, air cannot get into the piezometric tube and technical difficulty in measuring velocity of aerated flow is overcome.

3. 3-D flow feature in plunge pool

Figs. 3, 4 and 5 are the longitudinal, transverse and horizontal sections of the velocity vector field respectively in the Xiaowan plunge pool, with the calculated on the left-hand side and the measured on the right-hand side. The measured data are obtained

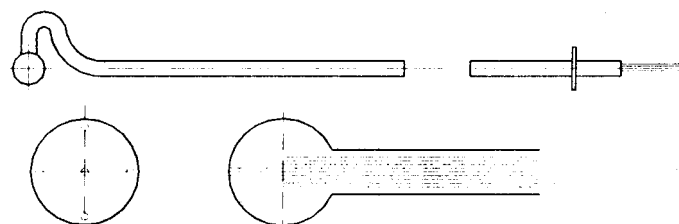
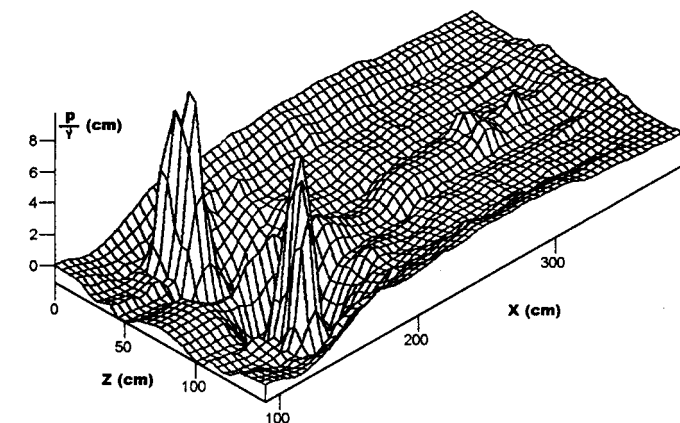
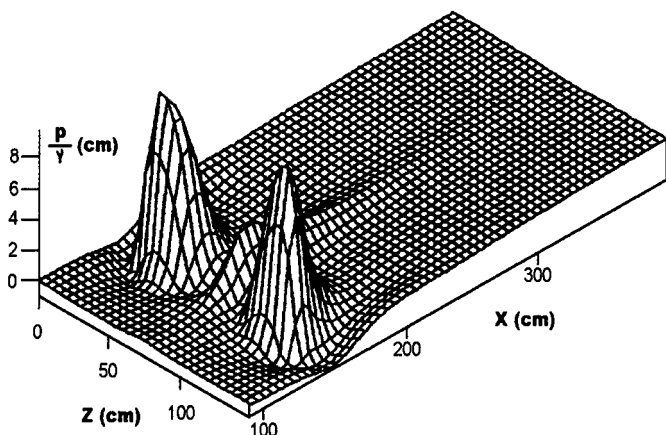


Fig. 2. The sketch of the five-hole Pitot sphere.



(A) The measured



(B) The calculated

Fig. 1. The comparison between the measured and the calculated pressure distributions on the floor

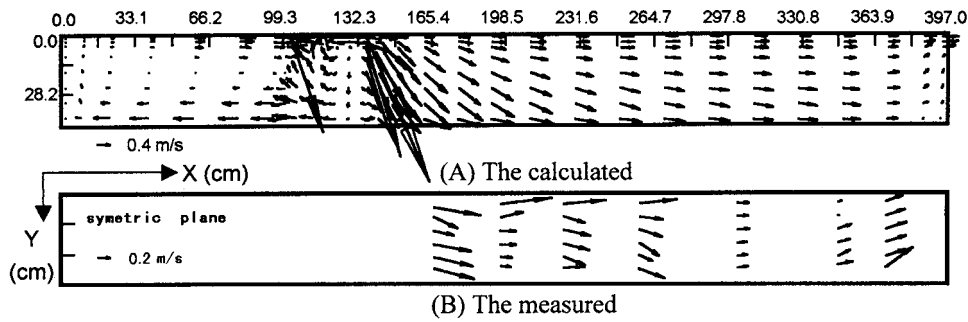


Fig. 3. Longitudinal section of flow field in plunge pool

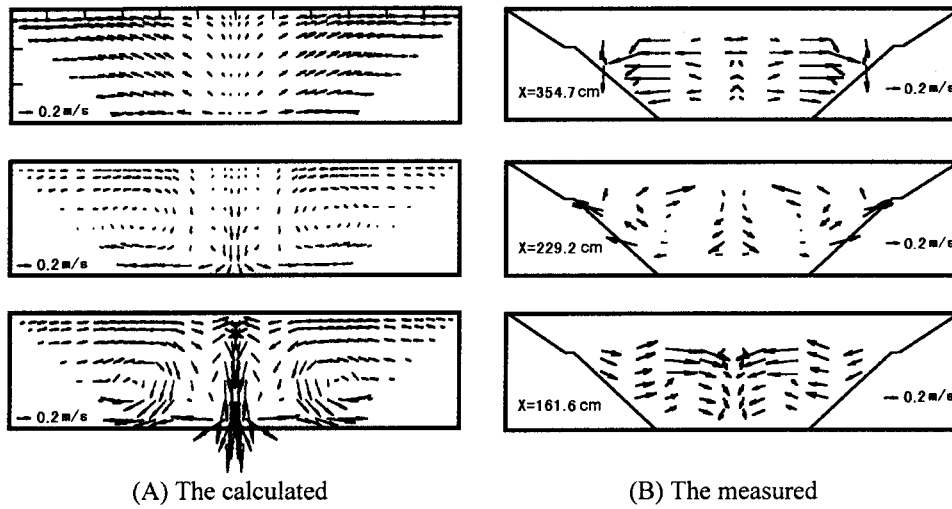


Fig. 4. Transverse sections of flow field in plunge pool

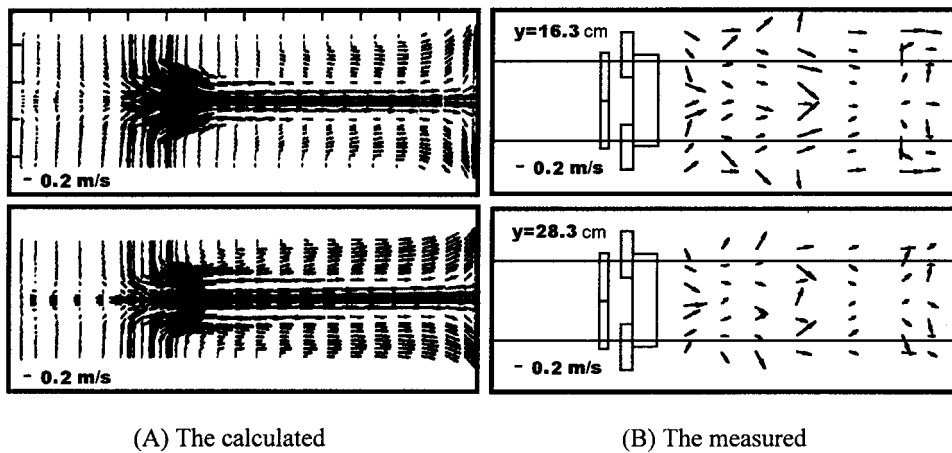


Fig. 5. Horizontal sections of flow field in plunge pool

from a physical model of 1:100, in which the width of the pool floor and the height of the end sill are respectively 70cm and 35cm. The side slope is 1:1.1. When flood is discharged through five top outlets at the normal flood level, the flow rate is 68.5 l/s and the water depth in the plunge pool is 42.3cm (in the model). The nappe consists of five streams, with the incident angles 65° ~ 69° and the profile as shown in Fig. 5b. Because of symmetry, only a half of the flow field is calculated and measured, and the whole flow field is given when the velocity vectors are plotted by microcomputer (see Figs. 4 and 5). On the basis of the calculated and measured results, the typical features of the 3-D flow in plunge pool can be obtained.

The velocity in the upstream and impact region of the incident point is difficult to measure and no recirculation appears in the measured region. However, the calculated results show a little recirculation near the incident point, as shown in longitudinal section in Fig.3. It is also shown that the range of recirculation relates to the angle of incidence, decreasing as the latter tends towards zero. In the upstream region of the incident point, as is shown by the calculated results, there is a large vortex. It can also be seen in the simulated results that the high speed jet changes direction abruptly near the bottom plate, which is consistent with the result that the calculated and measured hydrodynamic pressure on the bottom plate rises abruptly near the impact point and

drops to a gentler level on other part of the bottom plate. In the transverse sections (Fig.4), it can be seen from both the calculated and the measured results that there are two symmetric transverse circulations. It implies that the flow is spiral in the plunge pool. However, if the nappe were so wide as the width of the water surface, no space would be left for water to form transverse circulations, then the transverse circulations seen in Fig.4 would not exist. In some transverse sections, there are two smaller secondary circulations near the water surface. In the region near the end sill, the velocity vectors have radial distribution in the transverse section.

A plane view is given in Fig.5, showing that the transverse distribution of longitudinal velocity component has several peaks. The positions of the peaks are correspondent with those of the incident points, which can also be seen in the calculated results of Laxiwa plunge pool and therefore is of certain universality.

On the basis of the calculated and measured results, the typical pattern of the 3-D flow field in plunge pool is drawn in Fig. 6. The shape of water surface in the Xiaowan plunge pool is simulated by using the "elastic lid" method¹⁵ and also drawn in Fig. 6, which is in agreement with the experimental shape of the water surface.

The 3-D velocity field in the Laxiwa plunge pool was also calculated, but was not measured experimentally. Therefore, it is not

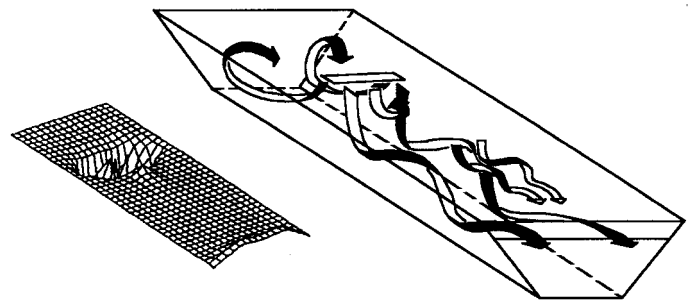


Fig. 6. Typical pattern of 3-D flow field in plunge pool

drawn in this paper.

4. Energy dissipation characteristics in plunge pool

Turbulent energy and its dissipation rate are the important factors reflecting the features of energy transition and exchange. The energy loss of jet from its impinging into plunge pool to its flowing out of the plunge pool is firstly turned into the turbulent energy from the time-averaged energy, then is dissipated as the heat energy due to the fluid viscosity. In fact, the energy dissipation is the process of energy transferring and exchanging.

The distributions of turbulent energy in the horizontal planes are

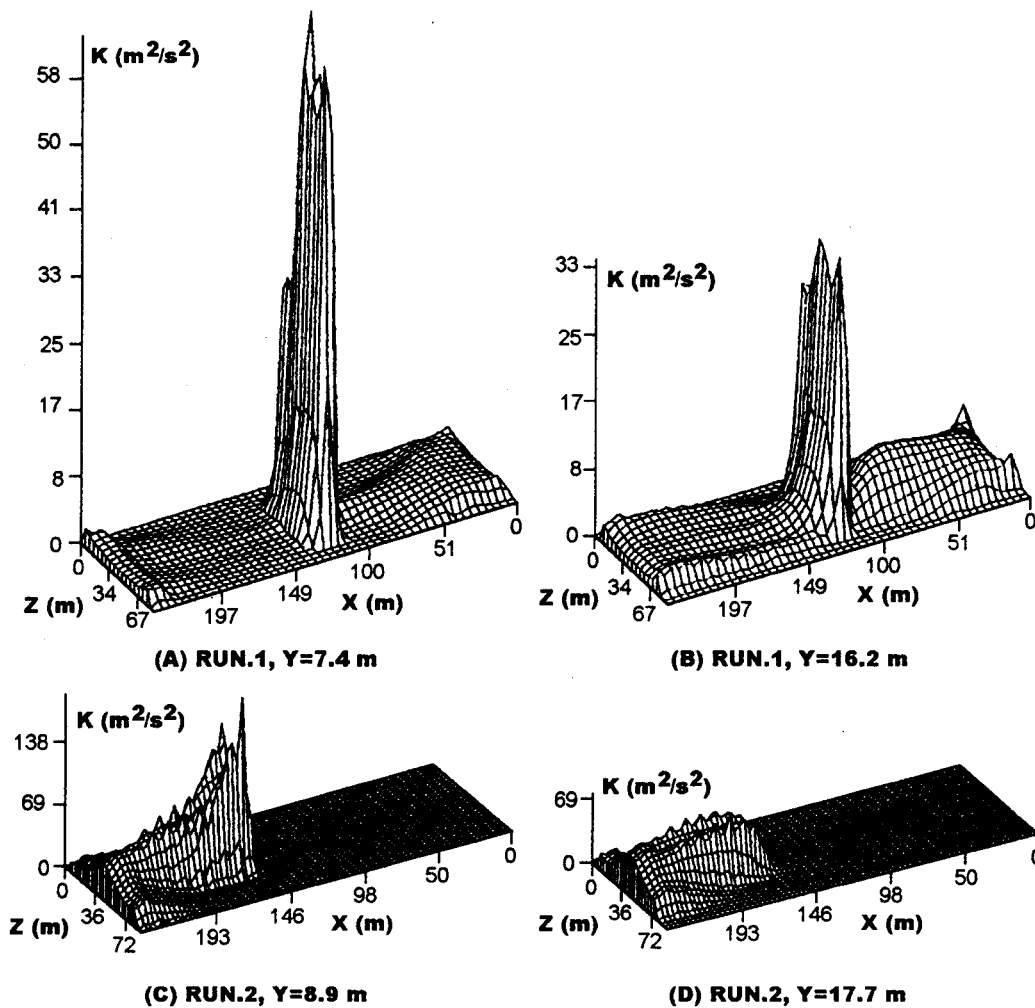


Fig. 7. Distribution of turbulent energy

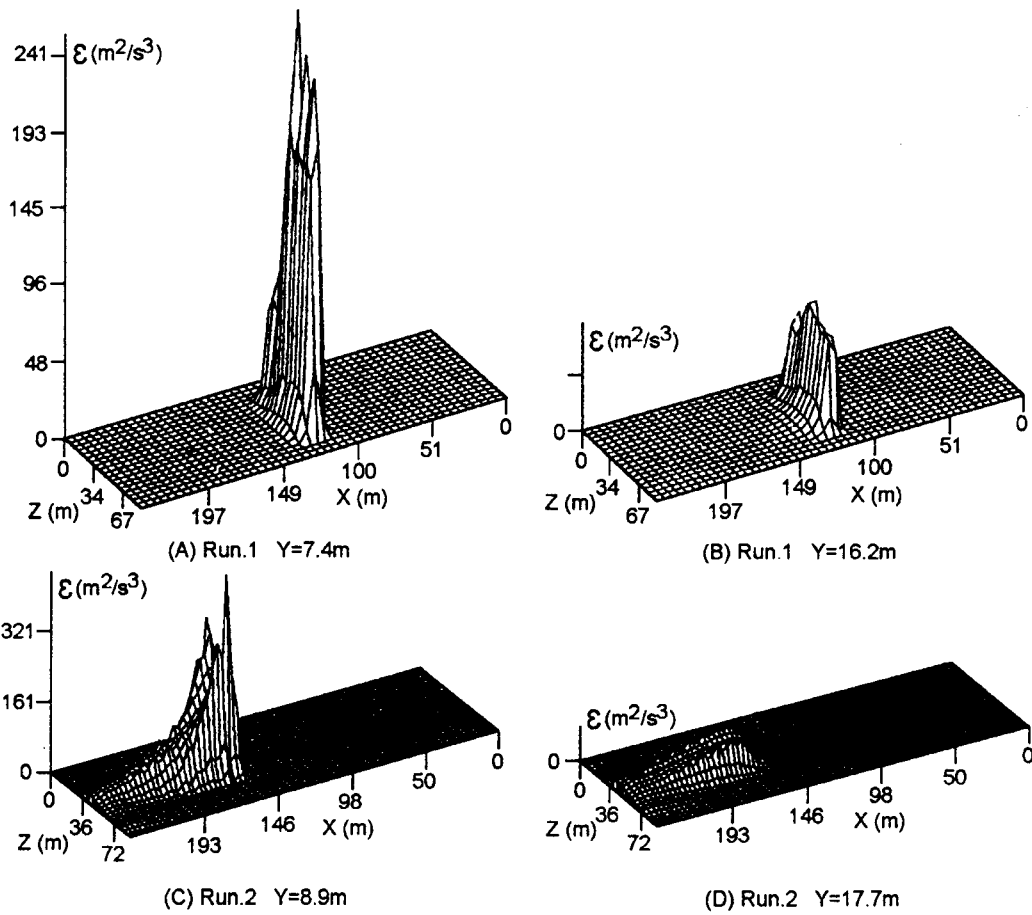


Fig. 8. Distribution of turbulent energy dissipation rate

shown in Fig. 7 and those of turbulent energy dissipation rate are shown in Fig. 8 (two representative runs of the Laxiwa plunge pool). It can be seen in the figures that the turbulent energy and its dissipation rate mainly concentrate near the jet axis, especially the dissipation rate. Table 1 shows the percentages of the turbulent energy and dissipation rate in the regions near the jet axis over those in whole plunge pool (Fig.9 is a sketch to show the region used for the calculation of k and ϵ , where L is the length of the plunge pool and α is the percentage of the water volume as shown in Table 1). The results shown in Table 1 indicate again that the energy transition occurs mainly in the region near the jet axis and only a little of water mass in the plunge pool takes part in the energy dissipation. This reveals one of the reasons why the more concentrated the jets, the more difficult the energy dissipation. On the other hand, it can also be seen in the distributions of turbulent energy and its dissipation rate that the maximum values of turbulent energy and dissipation rate appear at the position near

the water surface. The above-mentioned characteristics, together with the flow feature, show that the shear of water flow is the main dissipation mode in plunge pool when the water depth is enough (the smaller the water depth, the less the shear dissipation of energy). In the region near the incident point, where the shear of water flow is very obvious, large amount of energy is dissipated. Then, in the region where the jet impacts the pool floor, the energy is dissipated secondly by impacting. Before reaching the end sill, the energy is dissipated thirdly by turbulent mixing of water flow in the plunge pool. On the basis of the above-mentioned characteristics, the whole water body in plunge pool can be divided into three energy dissipation regions, i.e. shear, impact and mixing dissipation regions of energy, as shown in Fig. 10. The way of the optimization of plunge pool and dam outlets should be: expanding the range of the shear dissipation region

Table 1. Percentage of k and ϵ near the jet axis

Run No.	1	2	3	4	5	6
Percentage of volume of water body (%)	23	22	23	23	23	23
Percentage of k (%)	43	38	49	50	47	43
Percentage of ϵ (%)	90	65	89	88	85	88

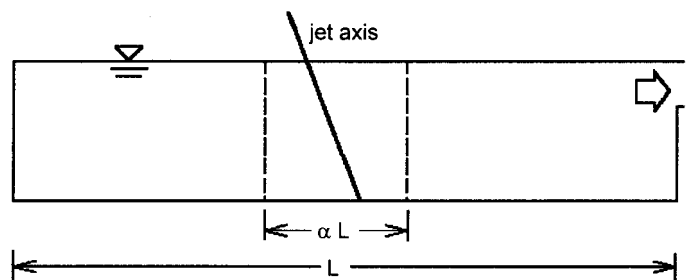


Fig. 9. Sketch of region used for the calculation of k and ϵ

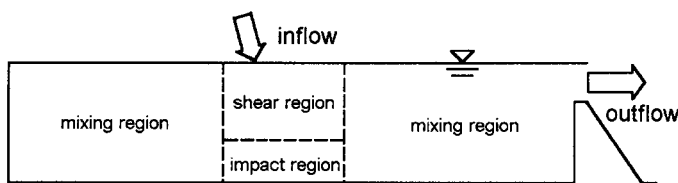


Fig. 10. Regions of energy dissipation in plunge pool

(e.g. dispersing the nappes), reducing the impact intensity in the impact dissipation region (e.g. forming moving water cushion), and making use of the water body in the mixing dissipation region as much as possible.

The calculated and the measured maximum pressures on the bottom plates of the two plunge pools are compared and the errors are equal to 4.9-7.8%, which shows reasonable agreement.

It should be noted that not only the maximum pressure but also the gradient of the pressure distribution on the pool floor should be restricted in the design of plunge pools. The large pressure gradient means that the shear dissipation is not enough and the impact kinetic energy is concentrated too much. Besides, the large pressure gradient may cause a very large lift force on the pool floor. The 3-D model in this paper can be used to compute the forces on the upward surface of the concrete slab, but the forces on the downward surface are very complex. Therefore, the limitations of the maximum kinetic pressure and the maximum pressure difference need to be determined empirically. An example of the limitation is: the maximum time-averaged kinetic pressure head is limited under 15m (as in the designs of the Ertan, the Xiaowan and the Xiluodu plunge pools); the difference between the maximum and the minimum time-averaged kinetic pressure heads is also limited under 15m. In order to decrease the pool depth as much as possible under the limited condition, the water flow should be divided into multiple jets and each jet should be dispersed enough before entering the plunge pool. Furthermore, it is a good choice that the upstream jet forms a moving water cushion under the downstream jet, which may decrease the impact force on the pool floor. It can be achieved by optimizing the distance between jets. In addition, because the water body between the jet entry location and the dam is quite stable and has very little action in energy dissipation, the distance between the jet entry location and the dam should not be too long so as to decrease the plunge pool length and increase the energy dissipation rate per unit volume in the plunge pool.

5. Conclusions

(1) The calculated and measured velocity field and the distribution of the turbulence parameters show the key flow features and energy dissipation characteristics in plunge pool. The typical pattern of the 3-D flow field and the division of the energy dissipation regions are very useful for understanding the turbulent flow characteristics in plunge pool.

(2) The way of the optimization of plunge pool and dam outlets should be to expand the range of the shear dissipation region (e.g. dispersing the nappes), reduce the impact intensity in the impact dissipation region (e.g. forming moving water cushion), and make

use of the water body in the mixing dissipation region as much as possible.

(3) The combination of the 3-D numerical simulation and the advanced measuring technique is an effective way to study the flow feature and energy dissipation characteristics in plunge pool.

References

1. Rodi, W., "Turbulence models and their application in hydraulics", IAHR Publication, Delft, The Netherlands, April, 1980:27-30.
2. Launder, B.E., Reece, G.J. and Rodi, W., "Progress in the development of a Reynolds stress turbulence closure", J. Fluid Mech., Vol.68, 1975:537-566.
3. Lesieur, M. And Metais, O., "New trends in Large-Eddy Simulations of turbulence", Annual Review of Fluid Mechanics, Vol.28, 1996:45-52.
4. Chen Yongchan et al. "Numerical simulation of the characteristics of free overfall jets in downstream scour hole", J. Hydraulic Engineering, No.4, 1993:48-54. (in Chinese)
5. Barata, J.M. et al. "On the analysis of impinging jet on ground effects", Experiments in Fluids, Vol.15, No.1, 1993:117-129.
6. Yang, Y.Q., Liao, H.S. and Xu, W.L., "Hydraulic characteristics and design optimization of the Xiaowan plunge pool", Research Report of Chengdu University of Science and Technology, April, 1998. (in Chinese)
7. Yang, Y.Q. and Xu, W.L., "Numerical simulation and energy dissipation analysis of the Laxiwa plunge pool", Research Report of Chengdu University of Science and Technology, Dec., 1997. (in Chinese)
8. Yang, Y.Q. and Xu, W.L., "Mathematical model of flood discharge and energy dissipation of the Xiluodu hydropower station", Research Report of Chengdu University of Science and Technology, June, 1997. (in Chinese)
9. Yang, Y.Q. and Xu, W.L., "Numerical simulation of the flow field in a plunge pool", Research Report of Chengdu University of Science and Technology, May, 1990. (in Chinese)
10. Dong, Z.Y., Yang, Y.Q. and Wu, C.G., "Influence of aeration on the pressure on the plunge pool bottom by jet impact", Science in China, Ser.A, Vol.24, No.4, 1994:431-439. (in Chinese)
11. Mason, P. J., "Effect of air entrainment on plunge pool scour", J. Hydraulic Engineering, ASCE, Vol.115, No.3, 1989:385-399.
12. Ervine, D.A., Falvey, H.T. and Withers, W.A., "Pressure fluctuations on plunge pool floors", J. Hydraulic Research, Vol.35, No.2, 1997:257-279.
13. Ervine, D.A. and Falvey, H.T., "Behavior of turbulent water jets in the atmosphere and in plunge pools", Proc. Instn. Civ. Engrs., Part 2, Vol.83, 1987:295-314.
14. McKeogh, E.J. and Elsayy, E.M., "Air retained in pool by plunging water jet", J. Hydraulics Division, ASCE, Vol.106, No.10, 1980:1577-1593.
15. Xu W.L., Yang, Y.Q., and Wu, C.G., "Numerical calculation of turbulent flow with free surface", J. Hydrodynamics, Ser.B, Vol.3, No.1, 1991:82-89.